How to cite: Angew. Chem. Int. Ed. 2024, e202317419
doi.org/10.1002/anie.202317419

Microplastic Degradation Hot Paper

Engineered Anchor Peptide LCI with a Cobalt Cofactor Enhances Oxidation Efficiency of Polystyrene Microparticles

Dong Wang, Aaron A. Ingram, Julian Luka, Maochao Mao, Leon Ahrens, Marian Bienstein, Thomas P. Spaniol, Ulrich Schwaneberg, and Jun Okuda**

Abstract: A typical component of polymer waste is polystyrene (PS) used in numerous applications, but degraded only slowly in the environment due to its hydrophobic properties. To increase the reactivity of polystyrene, polar groups need to be introduced. Here, biohybrid catalysts based on the engineered anchor peptide LCI_F16C are presented, which are capable of attaching to polystyrene microparticles and hydroxylating benzylic C–H bonds in polystyrene microparticles using commercially available oxone as oxidant. LCI peptides achieve a dense surface coverage of PS through monolayer formation within minutes in aqueous solutions at ambient temperature. The catalytically active cobalt cofactor **Co-L1** or **Co-L2** with a modified *NNNN* macrocyclic TACD ligand (TACD = 1,4,7,10-tetraazacyclododecane) is covalently bound to the anchor peptide LCI through a maleimide linker. Compared to the free cofactors, a 12- to 15-fold improvement in catalytic activity using biohybrid catalysts based on LCI_F16C was observed.

Global plastic pollution has fueled the quest for technological solutions to address the environmental impact of polymer waste.[1–4] Polystyrene (PS) is a plastic material that is widely used in many areas since the 1930s. A major drawback of polystyrene is its poor biodegradability, leading to pollution because mixed PS plastics waste and degradation products such as PS nano- and microparticles are difficult to be recycled in municipal recycling programs.[5–8] Due to its lack of polarity, PS is unreactive against many polar reactants.[9–11] To functionalize polystyrene, polar groups such as hydroxyl and carbonyl groups need to be introduced by selective C–H bond functionalization.

Anchor peptides (APs) are versatile adhesive peptides that can interact with a wide range of surfaces, including stainless steel and polymer surfaces[12] through multiple non-covalent interactions such as electrostatic, polar, hydrophobic, and hydrogen bonds.[13–15] As previously demonstrated, β-stranded anchor peptide LCI ("liquid chromatography peak I") showed specific and efficient binding to many polymer surfaces like polystyrene under mild conditions.[16–24] As one gram of anchor peptide is sufficient to coat a surface of up to 654 m^2 as monolayer,[25] anchor peptides offer a scalable, simple and cost-effective functionalization technology through spraying and dip coating.[25–28]

Organometallic catalysts allow selective C–H bond oxidation of small molecule alkanes by various oxidants,[29–41] but to limited extent of polyolefins. Hillmyer and co-workers have achieved the selective hydroxylation of methyl groups of branched polyethylene via rhodium-catalyzed alkane borylation, followed by oxidation of the resulting alkylboronate esters with hydrogen peroxide leading to alcohols.[42] The direct oxidation of polyethylene-*alt*-propylene (PEP) using oxone as oxidant was catalyzed by the manganese porphyrin complex Mn(TDCPP)OAc (TDCPP = *meso*-tetrakis(2,6-dichlorophenyl)porphyrin) in the presence of imidazole as phase transfer agent to provide the corresponding alcohols and ketones under mild conditions.[43] More recently, the iron-catalyzed oxyfunctionalization of polystyrene with chain cleavage using hydrogen peroxide as oxidant was reported.[44]

In this context, the improved binding of catalytically active metal species to a polymer molecule by conjugation with an anchor peptide holds promise to locate catalysts close to the polystyrene surface. We report here on biohybrid catalysts **Co-L1**@LCI_F16C and **Co-L2**@LCI_F16C based on an engineered anchor peptide LCI_F16C[16] that contain cobalt cofactors with the *NNNN* macrocyclic ligand TACD (TACD = 1,4,7,10-tetraazacyclododecane) through a linker and that catalyze C–H bond oxidation of polystyrene microparticles (MPs) using oxone as oxidant in aqueous solution.

Two cobalt complexes with maleimide linker **Co-L1** and **Co-L2** were prepared by reacting the corresponding macrocyclic ligand with cobalt dibromide in dichloromethane and characterized by elemental analysis, UV/Vis spectroscopy and ESI-TOF MS (for details see Supporting Information). The cobalt complexes **Co-L1** and **Co-L2** were covalently

[*] D. Wang, A. A. Ingram, Dr. T. P. Spaniol, Prof. Dr. J. Okuda
Institute of Inorganic Chemistry
RWTH Aachen University
Landoltweg 1, 52074 Aachen, Germany
E-mail: jun.okuda@ac.rwth-aachen.de
J. Luka, M. Mao, L. Ahrens, M. Bienstein, Prof. Dr. U. Schwaneberg
Institute of Biotechnology
RWTH Aachen University
Worringerweg 3, 52074 Aachen, Germany
E-mail: u.schwaneberg@biotec.rwth-aachen.de

attached to the cysteine residue of the anchor peptide LCI_F16C by a Michael addition reaction in Tris-HCl buffer (10 mM, pH 7.5, 50 mM NaCl) in the presence of 15 % of acetonitrile (Figure 1a). The anchor peptide LCI_F16C contains an AEF-linker, a Strep-tag, a 17x-helix spacer, a TEV protease cleavage site, and a F16C substitution (calculated molecular weight: $M = 9371.42$ g/mol). In order to prevent dimerization through disulfide bond formation, dithiothreitol (DTT) was used to reduce the disulfide bond to the thiol group and the excess DTT was removed by using HiTrap desalting column.

The structure of the biohybrid catalysts was calculated using YASARA software (Figure 1b–c) based on the solution structure of LCI (PDB ID: 2B9K[20]) and showed the orientation of the flexible conjugated cobalt cofactors. The conjugation efficiencies (determined by inductively coupled plasma atomic emission spectroscopy, ICP-AES, Table S4) of the cobalt cofactors in LCI_F16C were higher than 90 %, indicating that one cobalt ion per anchor peptide LCI_F16C was incorporated. Since the cobalt cofactors might be non-specifically bound to the peptide surface through non-covalent binding or other interactions, the bioconjugation yield was further confirmed by cysteine titration using a maleimide-bearing fluorescence indicator ThioGlo-1 (Figure S17). While free LCI_F16C solution showed a significantly increased fluorescence after addition of ThioGlo-1, the sample of **Co-L1**@LCI_F16C and **Co-L2**@LCI_F16C exhibited 10 % fluorescence, indicating a coupling efficiency of approximately 90 %. The biohybrid catalysts obtained were further characterized by ESI-TOF MS analysis (Figure S13–15 and Table S3 in the Supporting Information). The calculated mass for catalysts **Co-L1**@LCI_F16C ($m/z = 10{,}025$) and **Co-L2**@LCI_F16C ($m/z = 10{,}067$) was observed in the ESI-TOF MS spectra.

The structural integrity of the biohybrid catalysts at 25 °C was established by circular dichroism (CD) spectra in sodium phosphate buffer (NaPB, 100 mM, pH 8.0) with 15 % MeCN (v/v) through the characteristic minimum at λ = 210 nm (Figure 2, blue for **Co-L1**@LCI_F16C and red for **Co-L2**@LCI_F16C), which is similar to that of LCI_F16C (Figure 2, black).

Fluorescence-based characterization was achieved by labeling the polystyrene particles with plastibodies. Plastibodies are fluorescent peptides labeled or conjugated with material-specific binding properties that are comparable to binding properties of antibodies.[24] A Strep-tag-bearing fluorescence indicator Strep-Tactin®XT DY-549 (DY549), which showed a high affinity and specificity to the Strep-tag, was used. Characteristic absorption and emission maxima for DY549 were found at λ = 550–560 and λ = 575 nm, respectively. To generate the plastibodies, biohybrid catalysts (**Co-L1**@LCI_F16C and **Co-L2**@LCI_F16C) were incubated with DY549 in Tris-HCl buffer (50 mM, pH 8.0). Labeling of polystyrene MPs (1 μm) with plastibodies was performed by incubation of plastibodies (**Co-L1**@LCI_F16C-DY549 or **Co-L2**@LCI_F16C-DY549) in a suspension of polystyrene MPs at room temperature. The non-bound fluorescent molecules were removed from the particle surface by several cycles of washing in aqueous solution. Confocal fluorescence microscopy was used to visualize the labeling of polystyrene MPs with plastibodies. To compare the results, polystyrene MPs were incubated in Tris-HCl buffer (50 mM, pH 8.0) containing DY549. This control experiment showed no fluorescence under the microscope (Figure 3a), indicating that the fluorescence dye DY549 was completely removed from the particle surface and no unspecific binding of DY549 to the polystyrene particle surface occurred. In contrast, the labeled particles with plastibodies (**Co-L1**@LCI_F16C-DY549 or **Co-L2**@LCI_F16C-DY549) showed an intensive fluorescence in their corresponding excitation/emission fields under the microscope (Figure 3b–c), suggesting the successful labeling of polystyrene MPs with both plastibodies.

The biohybrid catalysts were used for the oxidation of *sec*-butylbenzene, a model unit of polystyrene, using 2.0 equiv. of oxone ($2KHSO_5 \cdot KHSO_4 \cdot K_2SO_4$) as oxidant in sodium phosphate buffer (100 mM, pH 6.0–8.0) with different cosolvents (Table 1). Under these conditions, 2-phenyl-2-butanol was formed in the presence of the biohybrid catalysts **Co-L1**@LCI_F16C or **Co-L2**@LCI_F16C. No products of oxidation at the β-position of *sec*-butylbenzene were

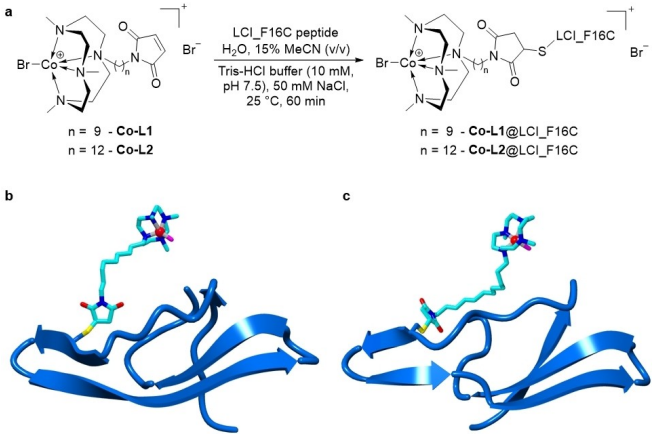

Figure 1. (**a**) Conjugation of cobalt cofactors to LCI_F16C. (**b**) Structure of **Co-L1**@LCI_F16C. (**c**) Structure of **Co-L2**@LCI_F16C. The structures were calculated based on the NMR spectroscopic solution structure of wild type LCI (PDB ID: 2B9K) and visualized with YASARA software.[45]

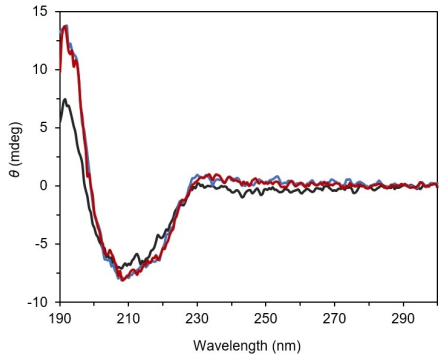

Figure 2. CD spectra of LCI_F16C (black), **Co-L1**@LCI_F16C (blue) and **Co-L2**@LCI_F16C (red) in sodium phosphate buffer (100 mM, pH 8.0).

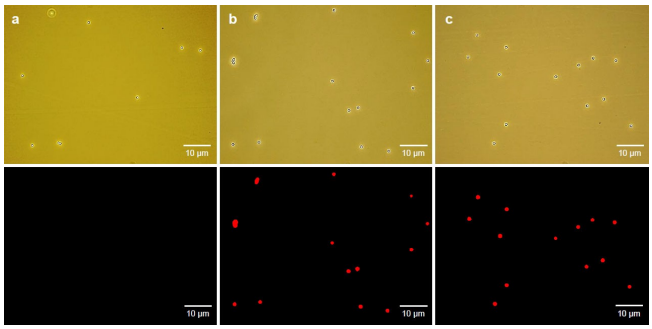

Figure 3. Visualization of polystyrene MPs (diameter = 1.0 µm) labeled with LCI_F16C-DY549 conjugates. The particles incubated with (**a**) DY549, (**b**) **Co-L1**@LCI_F16C-DY549, and (**c**) **Co-L2**@LCI_F16C-DY549 are visualized by bright-field (top) and fluorescence microscopy (bottom).

Table 1: Catalytic oxidation of *sec*-butylbenzene.

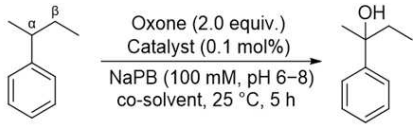

10 mM
1.0 equiv.

Entry	Catalyst	Co-solvent	pH	TON[a]
1	**Co-L1**@LCI_F16C	MeCN (15%)	6.0	55
2	**Co-L1**@LCI_F16C	MeCN (15%)	8.0	74
3	**Co-L1**@LCI_F16C	Acetone (15%)	8.0	30
4	**Co-L1**@LCI_F16C	THF (15%)	8.0	14
5	**Co-L1**@LCI_F16C	1,4-dioxane (15%)	8.0	17
6	**Co-L2**@LCI_F16C	MeCN (15%)	8.0	76
7[b]	**Co-L1**@LCI_F16C	MeCN (15%)	8.0	77
8[b]	**Co-L2**@LCI_F16C	MeCN (15%)	8.0	76
9[c]	**Co-L1**@LCI_F16C	MeCN (15%)	8.0	11
10	no catalyst	MeCN (15%)	8.0	<1

[a]Determined by GC-MS analysis. [b]16 h reaction time. [c]Reaction in Tris-HCl buffer (50 mM, pH 8.0).

observed. A comparison of entries 1 and 2 shows that the biohybrid catalysts are more catalytically active under basic conditions (pH 8.0) than under acidic conditions (pH 6.0). Oxidation using **Co-L1**@LCI_F16C and **Co-L2**@LCI_F16C with 15 % MeCN as cosolvent led to similar TONs of 74 and 76 in 5 h reaction time, respectively. Lower TONs were observed for the catalytic reactions with other cosolvents like acetone, THF, and 1,4-dioxane. Longer reaction time did not lead to higher TONs (Table 1, entries 7 and 8), indicating that the catalytic oxidation was complete within 5 h. The catalytic activity of **Co-L1**@LCI_F16C was much lower in Tris-HCl buffer (Table 1, entry 9), presumably as the result of demetalating the complex as well as by competing with substrate binding. The control reaction without catalyst showed that the oxidation of *sec*-butylbenzene with oxone at room temperature did not proceed (Table 1, entry 10).

The oxidation of polystyrene MPs (M_n = 38 kDa, determined by GPC analysis) with a diameter of 1 µm was carried out using **Co-L1**@LCI_F16C or **Co-L2**@LCI_F16C as catalyst with oxone as oxidant in sodium phosphate buffer (100 mM, pH 8.0) without any cosolvent. Taking into account the self decomposition of oxone over a period of 16 h, an excess amount of oxone (2.0 equiv.) with respect to the number of repeat units was used for the catalytic oxidation of polystyrene MPs. The suspension was stirred at room temperature for 16 h under argon atmosphere. The particles were then washed three times with distilled water and dried under vacuum for 16 h at 50 °C. To remove the water and the biohybrid catalyst completely, the product was dissolved in dry THF over activated molecular sieves (3 Å) and stirred for 24 h. The precipitated, denatured biohybrid catalyst was removed by filtration. The dry product was characterized by ESI-TOF MS to evaluate the leaching of the biohybrid catalyst. No corresponding peaks of the catalyst were observed in the mass spectrum, indicating that the catalysts were removed completely (Figure S16). The functionalized particles were subsequently characterized by ATR-IR spectroscopy. A broad band at ν = 3393 cm^{-1} corresponding to an O–H stretching frequency and a possible C–O stretching band at ν = 1194 cm^{-1} due to the tertiary alcohol were observed in the ATR-IR spectrum (Figure 4, blue), suggesting that hydroxyl groups were introduced into the polystyrene. As reported previously,[44] the C–O stretching absorption were observed in the oxy-functionalized polystyrene at ~1200 cm^{-1}, in addition to broad hydroxyl stretching bands at ~3400 cm^{-1}. The peaks of C–O and O–H stretching observed in this work are consistent with the reported data.

To quantify the functionalization level of polystyrene MPs, the functionalized polystyrene MPs were reacted with dansyl chloride (DsCl)[46–49] for the labeling of the hydroxyl groups formed by the catalytic oxidation reaction (Figure 5a). The calibration curve of dansyl chloride in

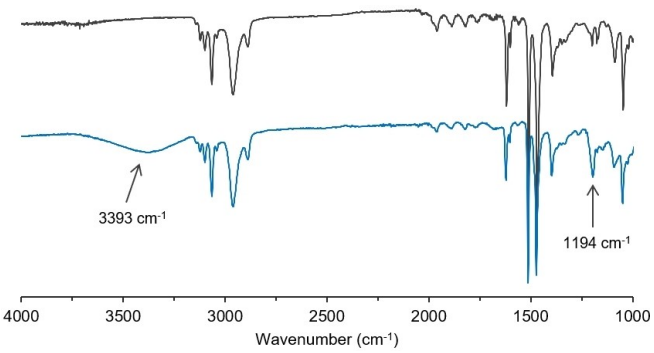

Figure 4. ATR-IR spectra of polystyrene MPs before (black) and after (blue) the oxidation catalyzed by **Co-L2**@LCI_F16C using oxone as oxidant.

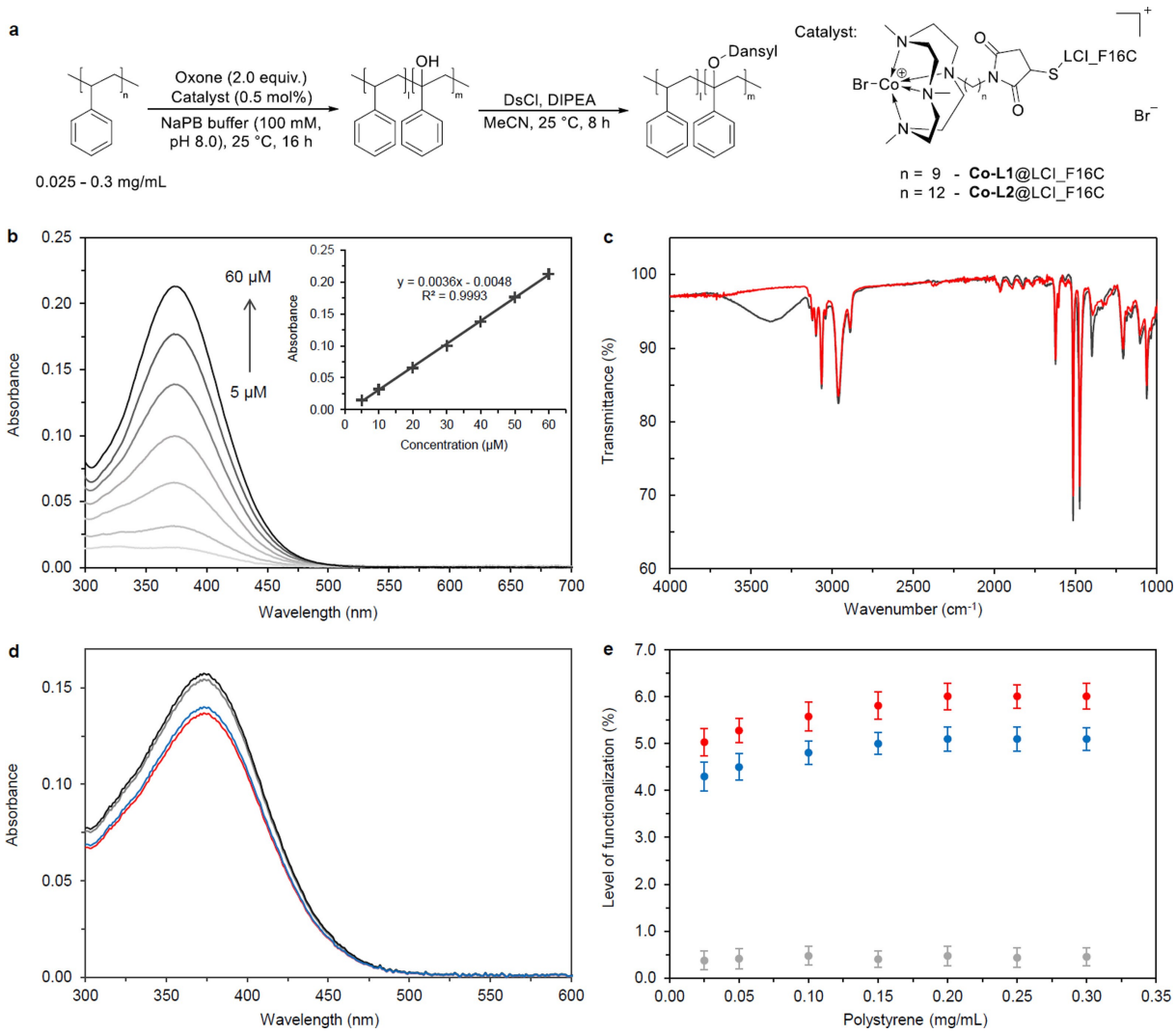

Figure 5. (**a**) Functionalization of polystyrene microparticles (1 µm) and labeling of the hydroxyl groups with dansyl chloride. (**b**) UV/Vis spectra of dansyl chloride in acetonitrile with concentrations from 5 to 60 µM. Inset: calibration curve at $\lambda = 375$ nm. (**c**) ATR-IR spectra of oxidized polystyrene MPs catalyzed by **Co-L2@**LCI_F16C before (black) and after (red) the reaction with dansyl chloride. (**d**) UV/Vis spectra of dansyl chloride solution in acetonitrile after the reaction with polystyrene MPs oxidized without catalyst (black), using **Co-L2** (grey), **Co-L1@**LCI_F16C (blue) and **Co-L2@**LCI_F16C (red) as catalyst. (**e**) Functionalization level of polystyrene MPs using **Co-L1@**LCI_F16C (blue), **Co-L2@**LCI_F16C (red) and **Co-L2** (grey) as catalyst.

acetonitrile showed an excellent R^2 value of 0.9993 (Figure 5b). After the reaction with dansyl chloride was complete, characterization of the polystyrene MPs by ATR-IR spectroscopy showed that the peak at $\nu = 3391\ cm^{-1}$ disappeared, indicating that the hydroxyl groups were completely consumed and labeled by dansyl chloride (Figure 5c, red). The absorbance at $\lambda = 375$ nm decreased significantly compared to the negative control (Figure 5d, black) after the dansyl chloride solution was treated with oxidized polystyrene MPs using **Co-L1@**LCI_F16C (Figure 5d, blue) or **Co-L2@**LCI_F16C (Figure 5d, red) as catalyst, while the absorbance decreased only slightly by reacting the dansyl chloride solution with polystyrene MPs oxidized by oxone using free cobalt cofactor **Co-L2** as catalyst (Figure 5d, grey). This clearly indicates that the oxidation of polystyrene MPs catalyzed by both biohybrid catalysts based on LCI_F16C anchor peptide led to a higher functionalization level than the reaction with free cobalt cofactor. The oxidation of polystyrene MPs was further optimized by varying the concentration of the particles in the range from 0.025 to 0.3 mg/mL (Figure 5e). The functionalization level increased from 5.0 % to 6.0 %, which corresponds to 60 hydroxyl groups per 1000 repeat units, when using **Co-L2@**LCI_F16C (Figure 5e, red) and from 4.3 % to 5.0 % using **Co-L1@**LCI_F16C (Figure 5e, blue) as catalyst, presumably because of stronger adhesion of the biohybrid catalyst to the particle surface at higher concentration. Further increase of particle concentration did not improve the functionalization level in case of oxidation reactions using both biohybrid catalysts, which indicates that the concentration of 0.2 mg/mL might be saturated for the adhesion of the biohybrid catalysts to polystyrene MPs. The higher functionalization level of

oxidized polystyrene MPs using **Co-L2**@LCI_F16C as catalyst than using **Co-L1**@LCI_F16C might be ascribed to higher flexibility of the cofactor **Co-L2**, which contains longer linker and should allow an increased probability to bind with the substrate. A 12-fold increase using **Co-L1**@LCI_F16C and a 15-fold increase using **Co-L2**@LCI_F16C as catalyst in the functionalization level compared to the use of the cobalt cofactor **Co-L2** (Figure 5e, grey) showed the significant influence of LCI_F16C anchor peptide to the oxidation of polystyrene MPs.

The GPC chromatogram of functionalized polystyrene MPs obtained by using **Co-L2**@LCI_F16C as catalyst showed that the distribution of the molar mass did not change significantly after the functionalization (Table S2), indicating that no chain cleavage occurred.

In conclusion, the combination of material-specific binding properties of the LCI peptide with a cobalt cofactor allowed to boost PS hydroxylation as initial step of its degradation by anchoring the cobalt cofactors to the PS surface as documented by confocal fluorescence microscopy. More specifically, biohybrid catalysts **Co-L1**@LCI_F16C and **Co-L2**@LCI_F16C based on the engineered anchor peptide LCI_F16C with flexible cobalt cofactors have been developed that hydroxylated polystyrene microparticles using commercially available oxone as oxidant. The oxidation of PS microparticles using both biohybrid catalysts showed 12–15 times higher functionalization level than using the free cobalt cofactors. It is very likely that the general concept of polymer degrading biohybrid catalysts can be expanded to hydrophobic polymers such as PP or even PE owning to LCI's binding properties. Through coating at ambient temperature, the biohybrid catalysts for polymer degradation reported here could be scalable and energy-efficient.

Supporting Information

The authors have cited additional references within the Supporting Information (Ref. [50–61]). Experimental procedures, spectroscopic characterization, and additional data are available in the Supporting Information.

Acknowledgements

We acknowledge the Bioökonomie REVIER_INNO PlastiQuant (FKZ: 031B0918E) and the German Federal Ministry of Education and Research (BMBF) for financial support. We thank Dr. G. Fink for assistance with NMR experiments and Dr. D. F. Sauer for helpful discussions. Open Access funding enabled and organized by Projekt DEAL.

Conflict of Interest

The authors declare no conflict of interest.

Data Availability Statement

The data that support the findings of this study are available from the corresponding author upon reasonable request.

Keywords: Anchor peptide · functionalized polystyrene · biohybrid catalysts · C–H bond activation · cobalt complex

[1] M. Sigler, *Water Air Soil Pollut.* **2014**, *225*, 2184.
[2] K. Duis, A. Coors, *Environ. Sci. Eur.* **2016**, *28*, 2.
[3] R. C. Hale, M. E. Seeley, M. J. La Guardia, L. Mai, E. Y. Zeng, *J. Geophys. Res. [Oceans]* **2020**, *125*, e2018JC014719.
[4] N. Parveen, V. P. Ranjan, S. Chowdhury, S. Goel, *Environ. Eng. Sci.* **2022**, *39*, 523–534.
[5] D. L. Kaplan, R. Hartenstein, J. Sutter, *Appl. Environ. Microbiol.* **1979**, *38*, 551–553.
[6] Y. Otake, T. Kobayashi, H. Asabe, N. Murakami, K. Ono, *J. Appl. Polym. Sci.* **1995**, *56*, 1789–1796.
[7] A.-C. Albertsson, S. Karlsson, *Int. Biodeterior. Biodegrad.* **1993**, *31*, 161–170.
[8] B. T. Ho, T. K. Roberts, S. Lucas, *Crit. Rev. Biotechnol.* **2018**, *38*, 308–320.
[9] S. M. Desai, R. P. Singh, *Long Term Properties of Polyolefins* (Ed.: A.-C. Albertsson), Springer Berlin Heidelberg, Berlin, Heidelberg, **2004**, pp. 231–294.
[10] C. W. S. Yeung, J. Y. Q. Teo, X. J. Loh, J. Y. C. Lim, *ACS Materials Lett.* **2021**, *3*, 1660–1676.
[11] S. Zeinali, M. Maleki, H. Bagheri, *J. Chromatogr. A* **2019**, *1602*, 107–116.
[12] Y. Ruan, M. Sohail, J. Zhao, F. Hu, Y. Li, P. Wang, L. Zhang, *ACS Biomater. Sci. Eng.* **2022**, *8*, 4738–4750.
[13] U. O. S. Seker, H. V. Demir, *Molecules* **2011**, *16*, 1426–1451.
[14] A. Care, P. L. Bergquist, A. Sunna, *Trends Biotechnol.* **2015**, *33*, 259–268.
[15] C. Liu, D. L. Steer, H. Song, L. He, *J. Phys. Chem. Lett.* **2022**, *13*, 1609–1616.
[16] L. Apitius, K. Rübsam, C. Jakesch, F. Jakob, U. Schwaneberg, *Biotechnol. Bioeng.* **2019**, *116*, 1856–1867.
[17] K. Rübsam, M. D. Davari, F. Jakob, U. Schwaneberg, *Polymer* **2018**, *10*, 423.
[18] K. Rübsam, L. Weber, F. Jakob, U. Schwaneberg, *Biotechnol. Bioeng.* **2018**, *115*, 321–330.
[19] M. Nöth, Z. Zou, I. El-Awaad, L. C. de Lencastre Novaes, G. Dilarri, M. D. Davari, H. Ferreira, F. Jakob, U. Schwaneberg, *Biotechnol. Bioeng.* **2021**, *118*, 1520–1530.
[20] W. Gong, J. Wang, Z. Chen, B. Xia, G. Lu, *Biochem.* **2011**, *50*, 3621–3627.
[21] N. Büscher, G. V. Sayoga, K. Rübsam, F. Jakob, U. Schwaneberg, S. Kara, A. Liese, *Org. Process Res. Dev.* **2019**, *23*, 1852–1859.
[22] D. B. Gehlen, L. C. De Lencastre Novaes, W. Long, A. J. Ruff, F. Jakob, T. Haraszti, Y. Chandorkar, L. Yang, P. van Rijn, U. Schwaneberg, L. De Laporte, *ACS Appl. Mater. Interfaces* **2019**, *11*, 41091–41099.
[23] J. Zhao, Y. Ruan, Z. Zheng, Y. Li, M. Sohail, F. Hu, J. Ling, L. Zhang, *iScience* **2023**, *26*, 106823.
[24] W. Bauten, M. Nöth, T. Kurkina, F. Contreras, Y. Ji, C. Desmet, M.-Á. Serra, D. Gilliland, U. Schwaneberg, *Sci. Total Environ.* **2023**, *860*, 160450.
[25] K. Rübsam, B. Stomps, A. Böker, F. Jakob, U. Schwaneberg, *Polymer* **2017**, *116*, 124–132.
[26] A. R. Grimm, D. F. Sauer, T. Mirzaei Garakani, K. Rübsam, T. Polen, M. D. Davari, F. Jakob, J. Schiffels, J. Okuda, U. Schwaneberg, *Bioconjugate Chem.* **2019**, *30*, 714–720.

[27] G. M. Rodriguez, J. Bowen, D. Grossin, B. Ben-Nissan, A. Stamboulis, *Colloids Surf. B* **2017**, *160*, 154–160.
[28] T. Wasilewski, B. Szulczyński, W. Kamysz, J. Gębicki, J. Namieśnik, *Sensors* **2018**, *18*, 3942.
[29] J. F. Hartwig, M. A. Larsen, *ACS Cent. Sci.* **2016**, *2*, 281–292.
[30] M. Lin, C. Shen, E. A. Garcia-Zayas, A. Sen, *J. Am. Chem. Soc.* **2001**, *123*, 1000–1001.
[31] S.-M. Lu, C. Chen, C. Liu, R. Liu, J.-H. Chen, Z. Zhang, Z. Yang, *Org. Lett.* **2023**, *25*, 2264–2269.
[32] N. Komiya, S.-I. Murahashi, *Chem. Rec.* **2021**, *21*, 1928–1940.
[33] M. Costas, *Coord. Chem. Rev.* **2011**, *255*, 2912–2932.
[34] B. R. Cook, T. J. Reinert, K. S. Suslick, *J. Am. Chem. Soc.* **1986**, *108*, 7281–7286.
[35] A. B. Sorokin, *Chem. Rev.* **2013**, *113*, 8152–8191.
[36] E. G. Chepaikin, *J. Mol. Catal. A* **2014**, *385*, 160–174.
[37] A. E. Shilov, G. B. Shul′pin, *Chem. Rev.* **1997**, *97*, 2879–2932.
[38] A. Sivaramakrishna, P. Suman, E. Veerashekhar Goud, S. Janardan, C. Sravani, T. Sandeep, K. Vijayakrishna, H. S. Clayton, *J. Coord. Chem.* **2013**, *66*, 2091–2109.
[39] P. Gandeepan, T. Müller, D. Zell, G. Cera, S. Warratz, L. Ackermann, *Chem. Rev.* **2018**, *119*, 2192–2452.
[40] H.-M. Shen, L. Liu, B. Qi, M.-Y. Hu, H.-L. Ye, Y.-B. She, *J. Mol. Catal.* **2020**, *493*, 111102.
[41] B. Wang, Y. M. Lee, W. Y. Tcho, S. Tussupbayev, S. T. Kim, Y. Kim, M. S. Seo, K. B. Cho, Y. Dede, B. C. Keegan, T. Ogura, S. H. Kim, T. Ohta, M. H. Baik, K. Ray, J. Shearer, W. Nam, *Nat. Commun.* **2017**, *8*, 14839.
[42] Y. Kondo, D. García-Cuadrado, J. F. Hartwig, N. K. Boaen, N. L. Wagner, M. A. Hillmyer, *J. Am. Chem. Soc.* **2002**, *124*, 1164–1165.
[43] N. K. Boaen, M. A. Hillmyer, *Macromolecules* **2003**, *36*, 7027–7034.
[44] S. McArthur, M. C. Baird, *Eur. Polym. J.* **2014**, *55*, 170–178.
[45] E. Krieger, G. Koraimann, G. Vriend, *Proteins Struct. Funct. Bioinf.* **2002**, *47*, 393–402.
[46] R. Bartzatt, *J. Biochem. Biophys. Methods* **2001**, *47*, 189–195.
[47] A. Salanti, M. Orlandi, L. Zoia, *ACS Sustainable Chem. Eng.* **2020**, *8*, 8279–8287.
[48] A. Sasaki, H. Aoshima, S. Nagano, T. Seki, *Polym. J.* **2012**, *44*, 639–645.
[49] Z. Tang, F. P. Guengerich, *Anal. Chem.* **2010**, *82*, 7706–7712.
[50] M. Wang, W.-W. Bao, W.-Y. Chang, X.-M. Chen, B.-P. Lin, H. Yang, E.-Q. Chen, *Macromolecules* **2019**, *52*, 5791–5800.
[51] D. Mukherjee, J. Okuda, *Chem. Commun.* **2018**, *54*, 2701–2714.
[52] E. Krieger, G. Vriend, *Bioinformatics* **2014**, *30*, 2981–2982.
[53] D. A. Case, V. Babin, J. Berryman, R. M. Betz, Q. Cai, D. S. Cerutti, T. E. Cheatham Iii, T. A. Darden, R. E. Duke, H. Gohlke, A. W. Goetz, S. Gusarov, N. Homeyer, P. Janowski, J. Kaus, I. Kolossváry, A. Kovalenko, T. S. Lee, S. LeGrand, T. Luchko, R. Luo, B. Madej, K. M. Merz, F. Paesani, D. R. Roe, A. Roitberg, C. Sagui, R. Salomon-Ferrer, G. Seabra, C. L. Simmerling, W. Smith, J. Swails, R. C. Walker, J. Wang, R. M. Wolf, X. Wu, P. A. Kollman, *Amber 14*, University of California, **2014**.
[54] A. Onoda, K. Fukumoto, M. Arlt, M. Bocola, U. Schwaneberg, T. Hayashi, *Chem. Commun.* **2012**, *48*, 9756–9758.
[55] K. Fukumoto, A. Onoda, E. Mizohata, M. Bocola, T. Inoue, U. Schwaneberg, T. Hayashi, *ChemCatChem* **2014**, *6*, 1229–1235.
[56] J. Wang, R. M. Wolf, J. W. Caldwell, P. A. Kollman, D. A. Case, *J. Comput. Chem.* **2004**, *25*, 1157–1174.
[57] A. Jakalian, D. B. Jack, C. I. Bayly, *J. Comput. Chem.* **2002**, *23*, 1623–1641.
[58] D. Wang, A. A. Ingram, A. Okumura, T. P. Spaniol, U. Schwaneberg, J. Okuda, *Chem. Eur. J.* **2023**, e202303066.
[59] C. Hirschhäuser, J. Velcicky, D. Schlawe, E. Hessler, A. Majdalani, J.-M. Neudörfl, A. Prokop, T. Wieder, H.-G. Schmalz, *Chem. Eur. J.* **2013**, *19*, 13017–13029.
[60] R. Sauer, P. Froimowicz, K. Schöller, J.-M. Cramer, S. Ritz, V. Mailänder, K. Landfester, *Chem. Eur. J.* **2012**, *18*, 5201–5212.
[61] M. J. Pfammatter, V. Siljegovic, T. Darbre, R. Keese, *Helv. Chim. Acta* **2001**, *84*, 678–689.

Manuscript received: November 16, 2023
Accepted manuscript online: January 22, 2024
Version of record online: ■■, ■■

Communications

Microplastic Degradation

D. Wang, A. A. Ingram, J. Luka, M. Mao, L. Ahrens, M. Bienstein, T. P. Spaniol, U. Schwaneberg,* J. Okuda* _____ **e202317419**

Engineered Anchor Peptide LCI with a Cobalt Cofactor Enhances Oxidation Efficiency of Polystyrene Microparticles

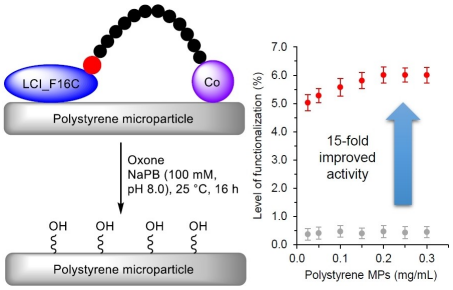

Engineered anchor peptide LCI_F16C with a flexible cobalt cofactor **Co-L2** hydroxylated polystyrene microparticles using commercially available oxone as oxidant. The oxidation using biohybrid catalyst (**Co-L2**@LCI_F16C) showed 15 times higher functionalization level than using the free cobalt cofactors.